Defect-related optical transitions in GaN

W. Rieger, R. Dimitrov, D. Brunner, E. Rohrer, O. Ambacher, and M. Stutzmann
Walter Schottky Institut, Technische Universität München, D-85748 Garching, Germany
(Received 26 August 1996)

Sub-band-gap absorption of GaN grown by metal-organic chemical vapor deposition on sapphire was investigated by photothermal deflection spectroscopy (PDS), transmission measurements, and the constant photocurrent method (CPM). We determine acceptor binding energies in undoped GaN at 220 and about 720 meV. A comparison between absorption and CPM spectra yields the dependence of the quantum efficiency-mobility-lifetime-product ($\eta\mu\tau$) versus energy and gives relevant information about the excitation mechanisms. CPM spectra show a significantly smaller absorption (up to a factor of 1/10) in the range between 3.0 and 3.3 eV as compared to PDS. This indicates that the majority of carriers excited with these photon energies have a relatively small $\eta\mu\tau$ product and thus do not contribute to the externally detected photocurrent. We propose that in this energy range the spectrum is dominated by interband absorption in isolated cubic-phase crystallites in the hexagonal matrix and by excitation of electrons from occupied acceptors into the conduction band of the main hexagonal crystal modification (h-GaN). Temperature-dependent photoluminescence measurements, excited with energies below and above the direct band gap of hexagonal GaN, confirm this interpretation and can be correlated with the subgap absorption detected by PDS. Transient photocurrent measurements show a persistent photoconductivity, which can also be explained by the existence of isolated cubic-phase inclusions. [S0163-1829(96)08048-4]

I. INTRODUCTION

In spite of recent successful developments in electronic[1–3] and optoelectronic[4,5] devices based on GaN, neither the density nor the microscopic origin of defects in this material is well understood so far. Future projects will focus on increasing the lifetime and mobility of carriers or minimizing parasitical sub-band-gap absorptions in GaN devices. Various defect spectroscopy methods can provide important contributions to this task. Low-temperature photoluminescence measurements[6–11] have most commonly been employed since the early 1970s to systematically study radiative transitions related to deep defects. More recently, photoemission capacitance transient spectroscopy,[12] deep-level transient spectroscopy,[13] and electron spin resonance[14] were also used to obtain further information on defect states in the gap of GaN. In addition to these techniques, subgap absorption studies with photothermal deflection spectroscopy[15] (PDS) and the constant photothermal method[16–18] (CPM) are also excellent methods for the investigation of gap states. Here, we present results from PDS, CPM, and photoluminescence (PL), Raman, and electrical measurements, which altogether give a consistent picture of defect-related optical transitions in GaN.

II. SAMPLE PREPARATION AND EXPERIMENTS

The GaN samples were grown by metal-organic chemical vapor deposition (MOCVD) on c-plane sapphire using triethylgallium (TEG) and ammonia at substrate temperatures of 950 °C.[19] To improve the structural properties of the films, a 20-nm-thick GaN buffer layer was grown at 530 °C. X-ray diffraction measurements were employed to characterize the crystal quality. The epitaxial films show a full width at half maximum (FWHM) of the rocking curve (002 reflex) of 300 arcsec. Contributions due to cubic inclusions are below the detection limit of approximately 1 vol %.

The total absorption coefficient is measured using photothermal deflection spectroscopy. In our PDS experiments a monochromatic light beam (chopped at 17 Hz) illuminates the GaN film (thickness d) immersed in a transparent liquid with a strongly temperature-dependent index of refraction $n(T)$. Part of the energy absorbed in the GaN diffuses back into the liquid and creates a temperature gradient and a corresponding refractive index gradient close to the sample surface. A He-Ne laser beam probes this gradient of n and is thus deflected ($\Delta\varphi$) periodically with the chopping frequency of the pump light. $\Delta\varphi(h\nu)$ is measured by a position-sensitive detector connected to a lock-in amplifier and can be expressed as[20,21]

$$\Delta\varphi(h\nu)\propto \delta n/\delta T\ \Phi\ h\nu(1-R)(1-e^{-\alpha(h\nu)d}), \qquad (1)$$

where Φ is the incident photon flux, $h\nu$ the photon energy, R the reflectivity of the sample surface, and $\alpha(h\nu)$ the absorption coefficient at the incident photon energy. This provides a very sensitive method for measuring the subgap absorption coefficient in thin GaN films:

$$\alpha(h\nu)=-\ln[1-\text{const}\times\Delta\varphi(h\nu)/\Phi h\nu]/d. \qquad (2)$$

In the limit of strong band-to-band absorption with $\alpha(h\nu)d$ greater than 1 the PDS signal $S_{\text{PDS}}\propto\Delta\varphi(h\nu)/\Phi h\nu$ saturates because all the incident light is absorbed by the GaN film. At this energy range ($h\nu>3.4$ eV, for GaN) no information about the absorption coefficient can be obtained from PDS. However, with the known thickness of the film, the onset of saturation can be used to determine the absolute absorption coefficient without the necessity for additional calibration. Thus, PDS spectra show the absolute value for $\alpha(h\nu)$ in the subgap energy range $h\nu<3.4$ eV (for GaN).

PDS experiments can be used to detect all transitions that absorb light and lead to nonradiative recombination. Since even in excellent semiconductor materials the quantum efficiency for radiative recombination at room temperature does not exceed a few percent, typically more than 90% of the absorbed energy is left to be detected by PDS.

In contrast to the PDS method described above, the constant photocurrent method is only sensitive to absorption processes, which generate mobile carriers. In a CPM measurement, the photocurrent j_{CPM} is kept constant by suitable adjustment of the incident photon flux Φ for different $h\nu$. The measured photocurrent j_{CPM} can be expressed as

$$\mathrm{const}=j_{\mathrm{CPM}}\propto e\,\eta\mu\tau\Phi(1-R)(1-e^{-\alpha(h\nu)d})E, \qquad (3)$$

where e is the elementary charge, η the quantum efficiency for optical generation of a mobile charge carrier, $\mu\tau$ the mobility-lifetime product, and E the applied electrical field. By keeping the photocurrent constant, the quasi-Fermi-level position and therefore the occupation of defects in the gap remains unchanged over the entire spectral range. In this case the lifetime τ should be constant. An effective absorption coefficient α_{CPM} can then be deduced from the constant photocurrent via the relation

$$\alpha_{\mathrm{CPM}}(h\nu)\propto -\ln(1-\mathrm{const}'/\Phi) \qquad (4)$$

and for $\mathrm{const}'\ll 1$:

$$\alpha_{\mathrm{CPM}}(h\nu)\propto \mathrm{const}'/\Phi. \qquad (5)$$

In general α_{CPM} depends on $\eta\mu(h\nu)$ and may differ significantly from α as determined, e.g., by PDS.

In undoped GaN (n-type, $n_e\approx 10^{17}$ cm^{-3}), the Fermi level is close to the conduction band and both the dark current and the photocurrent are dominated by electron transport. Therefore j_{CPM} is not sensitive to optical transitions, which do not lead to mobile electrons in the conduction band. Excitation of carriers into final states with recombination lifetimes much shorter than the lifetimes of the free carriers, or excitation in regions with low mobility (such as surface or interface regions) also do not contribute to the detected photocurrent. Photogenerated excitons that are not separated into free carriers are an additional absorption channel not seen by CPM. As a result, the true absorption coefficient α determined by PDS is expected to exceed α_{CPM} at any given photon energy.

The dependence of the mean $\eta\mu\tau$ value on the incident photon energy $h\nu$ can be obtained from the ratio $\alpha_{\mathrm{CPM}}/S_{\mathrm{PDS}}$:

$$S_{\mathrm{PDS}}(h\nu)=\Delta\varphi(h\nu)/\Phi h\nu\propto(1-R)(1-e^{-\alpha(h\nu)d}), \quad (1')$$

$$\eta\mu\tau\propto\mathrm{const}/\Phi[(1-R)(1-e^{-\alpha(h\nu)d})]^{-1}. \qquad (3')$$

Using (1′), (3′), and (5), we obtain

$$\eta\mu\tau(h\nu)\propto\alpha_{\mathrm{CPM}}(h\nu)/S_{\mathrm{PDS}}(h\nu). \qquad (6)$$

A comparison of both measurement techniques performed on the same samples therefore yields the dependence of $\eta\mu\tau$ on energy and gives additional information about optical excitation mechanisms in GaN.

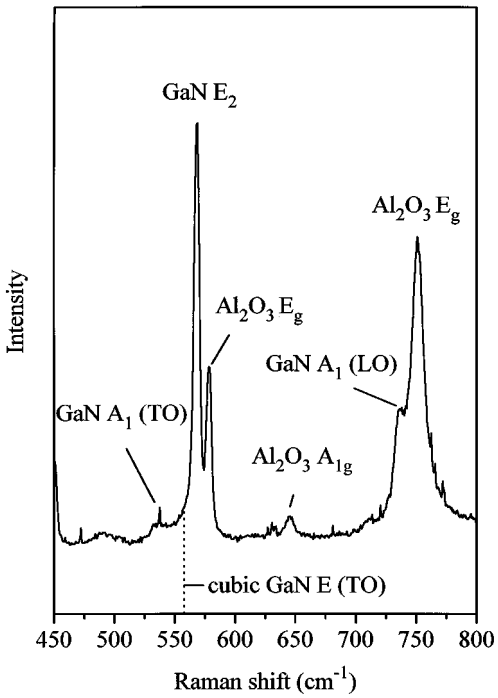

FIG. 1. Raman spectra of a 1-μm-thick GaN film measured at room temperature. The dashed line indicates where the transverse optical mode should occur in cubic GaN.

For photoluminescence measurements, the samples are mounted in a continuous flow cryostat. The temperature can be varied from 5 to 300 K. As an excitation light source two different UV lines of an Ar^+ laser (363.8 nm=3.41 eV and 333.6 nm=3.72 eV) were used. The luminescence light was detected with a 0.8-m double monochromator and a photomultiplier.

Raman measurements were performed using the 488-nm line of an Ar^+ laser (200 mW) in backscattering geometry. The scattered light was analyzed with a 0.8-m triple monochromator and a charge-coupled device camera. For macroscopic measurements, the spot size was about 400 μm in diameter. For micro-Raman measurements, the laser was focused through the objective of a microscope to a spot size of 10 μm. With both configurations several spectra were recorded, all showing the same features.

III. RESULTS AND DISCUSSION

Figure 1 shows a Raman spectrum of a 1-μm-thick GaN film. The well documented Raman modes of GaN (Ref. 22) and of the sapphire substrate are detected with a good signal-to-noise ratio. The dashed line indicates the energy position of the transverse optical mode in cubic GaN (555 cm^{-1}). The absence of any detectable signal indicates that the corresponding film consists to more than 99% of hexagonal GaN. Note, however, that in general x-ray diffraction measurements and Raman scattering are not sensitive enough to detect cubic phase inclusions of less than 1 vol % in typical h-GaN films.

Figure 2 shows the absorption coefficient α measured by PDS and CPM versus energy (solid line) of this sample on a logarithmic scale. To complement the PDS and CPM spectra in Fig. 2, the absorption was also determined from transmis-

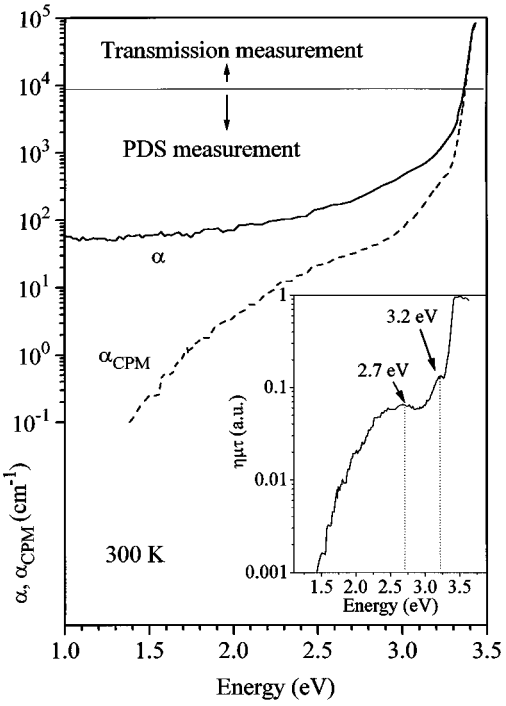

FIG. 2. Absorption coefficient α vs energy (solid) of a 1-μm-thick GaN film, on a logarithmic scale. To complement the PDS and CPM spectra, the absorption was also determined from transmission measurements ($h\nu > 3$ eV). The inset shows the ratio of α_{CPM} and S_{PDS} on a logarithmic scale. This expression is proportional to $\eta\mu\tau$ and depends on the number of mobile carriers per absorbed photon.

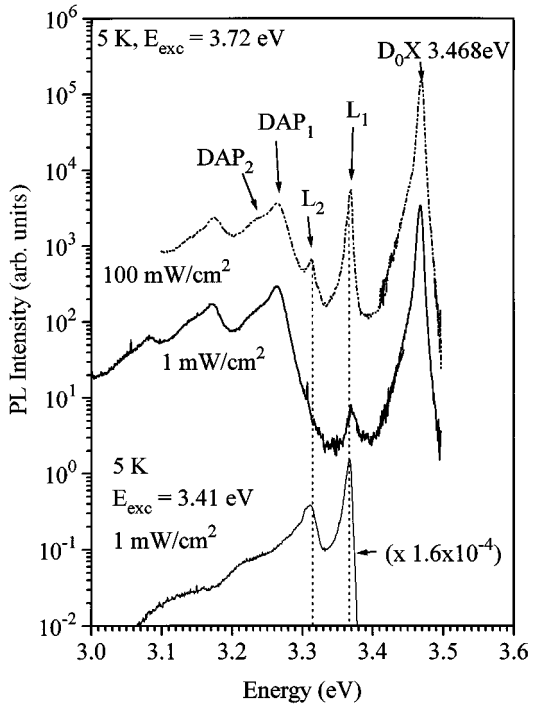

FIG. 3. A typical PL spectrum (solid line) for interband excitation ($E_{exc} = 3.72$ eV). The second spectrum (dashed) shows a PL spectrum for 100 times higher excitation intensity. For excitation photon energies below the band gap ($E_{exc} = 3.41$ eV), L_1 and L_2 completely dominate the photoluminescence (solid line, lower part).

sion measurements above 3 eV. The transmission and PDS results for α are in good agreement over about one order of magnitude. The result of the corresponding CPM measurement (dashed curve) is scaled to the α obtained from PDS and transmission at high energies. α and α_{CPM} agree nicely in the photon energy range between 3.3 and 3.4 eV, as expected for band-to-band transitions.

The inset in Fig. 2 shows $\alpha_{CPM}/S_{PDS} \propto \eta\mu\tau$ on a logarithmic scale. This quantity depends on the number of mobile carriers per absorbed photon. The observed features of the ratio were found to be independent of the particular value of j_{CPM} chosen. For photon energies above the direct gap, an almost constant and high $\eta\mu\tau$ value is obtained. The shoulder at 3.20 eV indicates electronic transitions from acceptors ($E_A = E_{gap} - 3.2$ eV$=220$ meV) into the conduction band. This transition takes place in the bulk material since the penetration depth is nearly equal to the thickness of the sample.

A particularly interesting energy range is around 3.30 eV, where the ratio shows a local minimum. This indicates a noticeably decreased $\eta\mu\tau$ product for the excited electrons. For a decreased mobility μ, the final state of the optical transition should be localized, with a low thermal activation probability into the conduction band at room temperature. This explanation requires the existence of unoccupied states well below the conduction band. Since the Fermi level of this sample is determined to be around 20 meV below E_C, which is typical for as-prepared GaN material, this scenario is rather unlikely. Another possibility would be a shorter lifetime τ of the excited electrons in comparison with the free-electron lifetime. This requires an additional, distinct recombination channel and cannot be ruled out. A third explanation is that surface or interface-related defect absorption dominates α at theses photon energies. In surface regions, a higher defect density leads to lower mobility and carrier lifetime and thus quenches the photocurrent. The energetic position of the minimum around 3.30 eV, in comparison with the optical band gap at 3.42 eV, points to a transition from an occupied acceptor ($E_A = 120$ meV at room temperature) into the conduction band, or from an occupied acceptor into a vacant shallow donor ($E_D + E_A = 120$ meV, $E_D < 20$ meV, at room temperature). This would correlate with donor-acceptor-pair transitions (DAP) pair transitions at 3.25–3.3 eV, which commonly are observed in low-temperature photoluminescence measure- ments.[7,9,11,23,24,25] The creation of deeply bound excitons would be another absorption channel with a low $\eta\mu\tau$ product of the corresponding photocurrent. The most probable creation path of such deeply bound excitons is via localization of free excitons. The optical cross section for the direct excitation of these excitons by sub-band-gap photon energies should be negligible.

A dominant structure in the low-energy part of the $\eta\mu\tau$ spectrum is a broad peak centered around 2.7 eV. This points to a density distribution of deep acceptors ($E_A \geq 3.42 - 2.7$ eV$=0.72$ eV). Such deep acceptors are commonly believed to be the origin of the ''yellow luminescence''.[26]

We now compare the absorption features to photoluminescence results of the same samples. A typical PL spectrum is shown in Fig. 3 (solid line) for band-to-band excitation ($E_{exc} = 3.72$ eV). It is dominated by the bound exciton transition D_0X (3.468 eV). The two weak lines L_1 and L_2 at

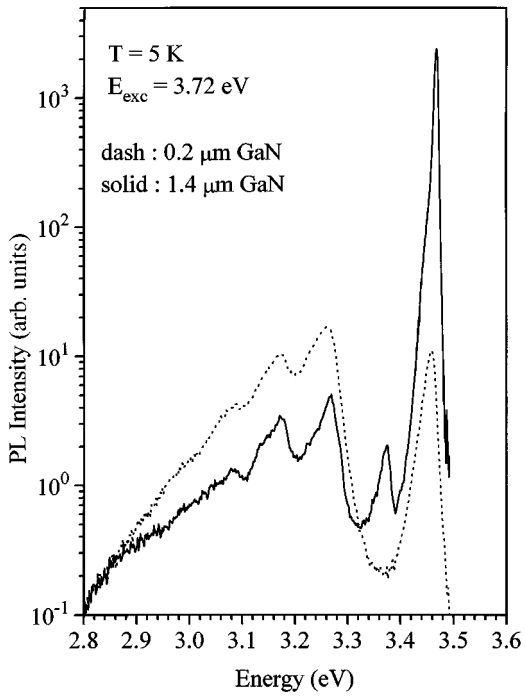

FIG. 4. Photoluminescence measurements made on GaN samples with two thicknesses (0.2 μm: dashed, 1.4 μm: solid, both on a 20-nm low-temperature GaN buffer layer) grown under the same deposition conditions.

3.369 and 3.313 eV were recently assigned to deeply bound excitons in structurally distributed regions[27] or to near-band-gap emission[28] in cubic GaN. In fact L_1 and L_2 consist of more than one single line. The respective intensity depends on excitation intensity and excitation wavelength, which lead to changed lines shapes for different experimental setups. As detailed below we believe that in our case cubic inclusions in a hexagonal matrix, probably caused by stacking faults,[29] are indeed the dominant origin for these PL lines.

The structure in the PL spectra occurring between 3.0 and 3.28 eV is generally labeled as DAP_1 and DAP_2 transitions with two LO-phonon replica. A second spectrum including L_1,L_2 and the DAP's is also shown in Fig. 3 for a 100 times higher pump intensity. We observe a distinct increase in the relative photoluminescence intensities of L_1 and L_2. Finally, for excitation photon energies below the band gap of h-GaN ($E_{\mathrm{exc}}=3.41$ eV), L_1 and L_2 completely dominate the photoluminescence. In fact the quantum efficiency η_{PL}(=emitted photons/absorbed photons) for L_1 ($E_{\mathrm{exc}}=3.41$ eV) is about 5 times higher than η_{PL} for the D_0X with excitation at $E_{\mathrm{exc}}=3.72$ eV. This is an important observation suggesting that L_1 and L_2 excitation does not require interband transitions in the hexagonal phase, but supports near-band-gap emission from cubic material as the origin of these lines.

In order to determine which transitions contribute to the structure in the subgap absorption spectra at room temperature (Fig. 2), more PL measurements were performed. Figure 4 shows photoluminescence measurements made on GaN samples with two thicknesses (0.2 and 1.4 μm) grown under equivalent conditions. Both are grown on the same 20-nm-thick low-temperature GaN buffer layer. The penetration depth of the excitation laser is below 100 nm. The spectrum

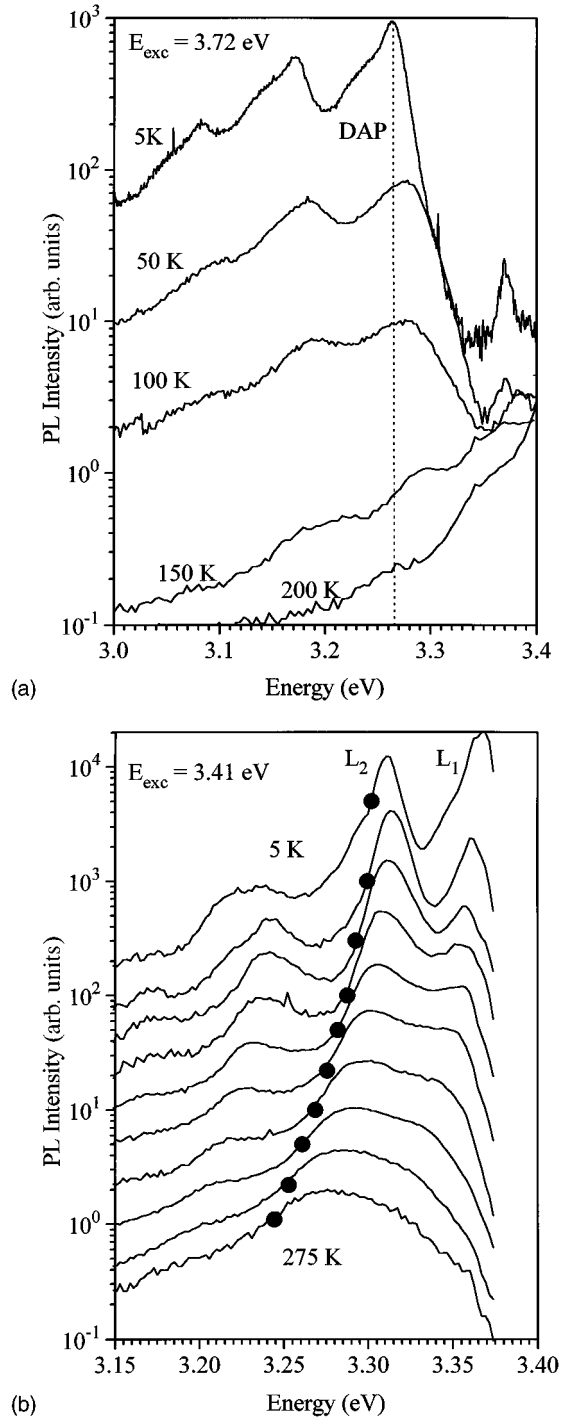

FIG. 5. The results of temperature-dependent PL measurements are shown vs energy [(a) interband excitation, (b) subband excitation]. The dots (b) indicate the temperature-dependent band gap of cubic GaN according to Ref. 31.

of the thin sample indicates an enhanced DAP luminescence, where the region of excitation is near the buffer layer. One possible explanation is a higher concentration of the relevant defects in the perturbed buffer region. The lower integral photoluminescence is probably caused by a higher concentration of deep nonradiative defects. Thus the DAP transitions in the buffer region are expected to contribute to subgap absorption without a noticeable creation of mobile

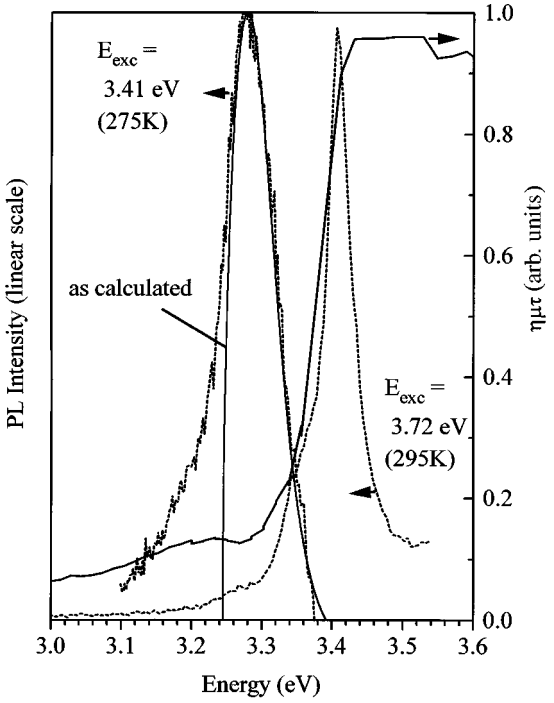

FIG. 6. In order to correlate the optical sub-band-gap absorption with radiative recombination excited above and below the hexagonal band gap, both $\eta\mu\tau$ at 295 K and two photoluminescence spectra are shown over the same energy range. The solid line, fitting the sub-band-gap excited PL, is calculated for occupied conduction-band states with a Fermi level 46 meV above E_c.

carriers. In the PL spectrum of the thicker sample L_1 is clearly visible.

Temperature-dependent measurements of a 1-μm-thick GaN sample are shown in Figs. 5(a) and 5(b). The DAP_1 and DAP_2 luminescence [Fig. 5(a)] is quenched with an activation energy of approximately 160 meV and is not visible at room temperature. The DAP_1 and DAP_2 positions shift to

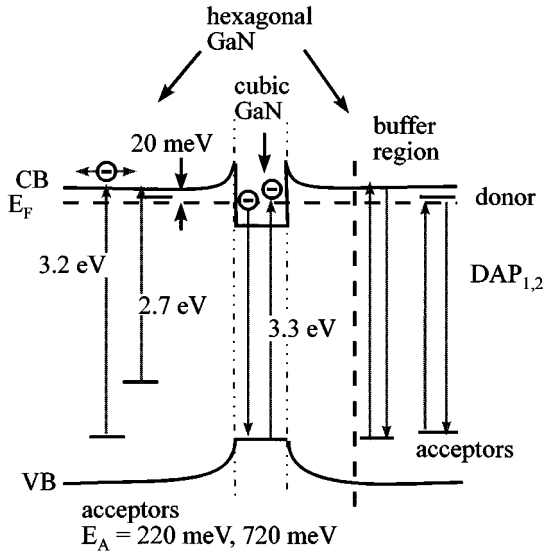

FIG. 7. Model summarizing the discussed mechanism of sub-band-gap absorption.

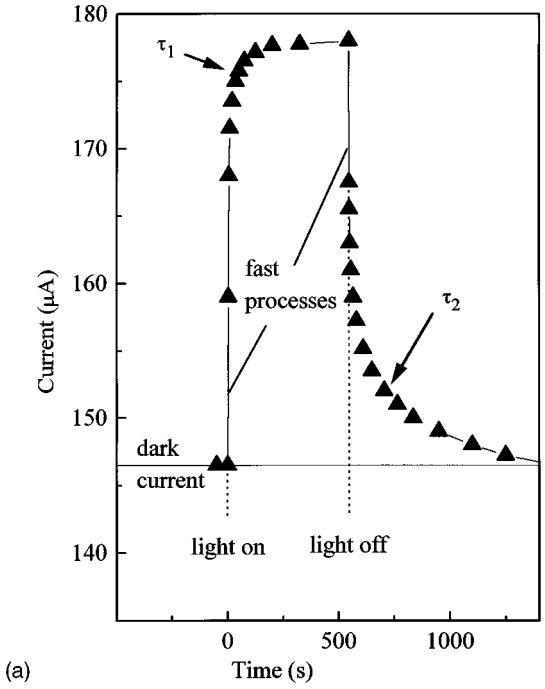

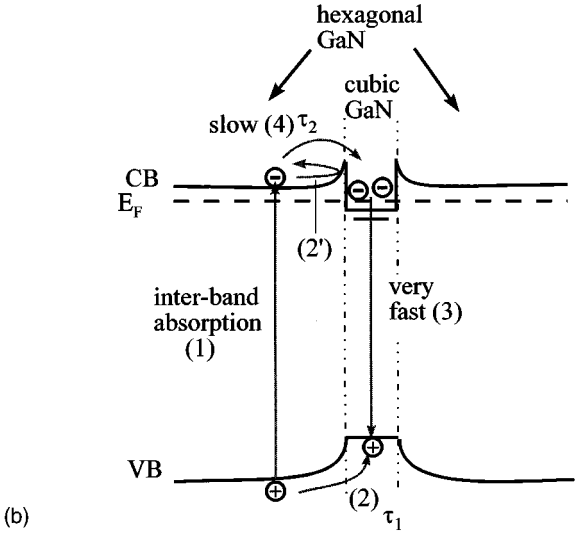

FIG. 8. Transient photoconductivity measurement performed on GaN. (b) Model for persistent photoconductivity.

higher energies with increasing temperature (3.285 eV at 200 K). This is in agreement with observations made by other groups.[9,25] The quenching points to thermal ionization of the donors (initial states) or thermal occupation of the acceptors (final states). As a result, the optical excitation from occupied acceptors into the conduction band or into shallow donors in bulk GaN is expected to contribute in photocurrent measurements at room temperature.

The intensity of the L_1 and L_2 transitions also decreases with higher temperatures [Fig. 5(b)], but can easily be observed with sub-band-gap excitation energies up to 275 K. At room temperature near-band-gap luminescence of the hexagonal GaN dominates the photoluminescence and covers these lines. An excitation of this near-band-gap luminescence becomes possible because the band-gap energy of hexagonal GaN (3.42 eV at 300 K) comes close to the excitation

energy of 3.41 eV for higher temperatures. The energy positions of L_1 and L_2 clearly show a decrease similar to the temperature-induced gap reduction. The dots in the figure indicate the temperature-dependent band gap of cubic bulk GaN according to Ref. 30, which is about 65 meV lower than L_1. This discrepancy is discussed later.

Thus the DAP_1, DAP_2, and L_1, L_2 transitions can be expected to participate in room-temperature defect absorption below 3.35 eV. In particular band transitions in cubic crystallites with a large optical cross section for excitation energies below the hexagonal band gap are a suitable explanation for a relatively lower value α_{CPM} at 3.30 eV. Such cubic regions embedded in the hexagonal matrix with a larger gap provide a sink for electrons and are thus negatively charged. The corresponding band bending results in a potential barrier and separates the electrons in the cubic part from the hexagonal matrix. A macroscopically detected current is therefore not influenced by optical transitions in cubic inclusions. On the other hand the electrons and holes are spatially confined and (radiative) recombination is very effective.

In order to demonstrate the correlation between the optical sub-band-gap absorption and radiative recombination excited above and below the hexagonal band gap, both $\eta\mu\tau$ at 295 K (calculated as discussed before) and photoluminescence spectra are shown in Fig. 6 over the same energy range. The PL spectra are in agreement with the band gaps of cubic[30,31] and hexagonal[31] GaN at room temperature. The slightly higher emission energy for the subgap-excited luminescence in comparison to the band-gap energy given in Ref. 30 (3.244 eV at 275 K) can be explained by band filling effects. The luminescence peak can easily be fitted (solid line) by a Fermi-level position 46 meV above the cubic conduction-band edge (3.29 eV), assuming band-to-band recombination. Integration up to 46 meV over a parabolic distribution density of states assuming a relative effective mass of $0.23m_0$ yield an electron concentration of 5×10^{18} cm^{-3}. Using this explanation, the origin of L_1, which occurs only at low temperatures, is not clear. Recombination of a free electron h-GaN with a hole bound to the crystallite may be one explanation.[32] In any case as shown in Fig. 6, the maximum of the subgap excited PL at 275 K coincides with the local minimum of $\eta\mu\tau$. Therefore the most reasonable explanation is that the optical absorption at 3.30 eV is dominated by interband transitions in cubic crystallites at room temperature. These transitions do not contribute to the macroscopic photocurrent. We can use the ratio of $\alpha(3.5\ \mathrm{eV})/\alpha(3.3\ \mathrm{eV})\approx100$ to determine the volume fraction of cubic GaN to $\leqslant1$ vol %.

The shoulder around 3.20 eV in the $\eta\mu\tau$ spectrum is caused by acceptor-conduction band transitions in bulk h-GaN. This yields an acceptor binding energy of $E_A=220$ meV. This energy is in good agreement with the residual acceptor binding energy of 230 meV given in Ref. 25 from an analysis in the DAP_1 and DAP_2 transitions. Optical excitation from these occupied acceptors lead to mobile electrons. Electron diffusion quenches the DAP luminescence (see Fig. 3 for $E_{\mathrm{exc}}=3.41$ eV). Very high concentrations of electrons and holes created with strongly absorbed light, especially in regions with low mobility, should produce strong DAP luminescence as seen in Fig. 4. In Fig. 7 a simple model is presented summarizing the discussed mechanism of sub-band-gap absorption.

More support for the existence of cubic inclusions in h-GaN and their relevance for the electronic properties of this material is shown in Fig. 8(a), which depicts a transient photoconductivity measurement performed on the same sample. Similar observations have already been described in Ref. 33. At $t=0$, monochromatic light (320 nm) is switched on to illuminate the sample surface between two coplanar Ohmic contacts. The current rises with a time constant of roughly 10 s and saturates after a few minutes. After 550 s the light is switched off and the current drops slowly. The decay time of this persistent photoconductivity is determined to about 60 s. Since the carrier lifetimes observed in GaN are below 1 ns, these long time constants cannot be explained by conduction-band transitions in hexagonal GaN. Such fast transitions may cause an additional part of the photoconductivity relaxation, which is not resolved on this time scale. We believe that spatial carrier separation, which is also observed in other III-V material systems,[34] is the reason for the persistent photoconductivity. In Fig. 8(b) our model is used to give a possible explanation: Interband absorption at room temperature creates a certain density of free carriers [Eq. (1)]. Some of the free carriers diffuse to cubic crystallites. In n-type GaN ($E_c-E_F\approx20$ meV), these cubic inclusions become negatively charged provided that the lower conduction-band minimum in c-GaN [$E_c(\mathrm{cubic})<E_c(\mathrm{hexagonal})$ by at least 66 meV$=20+46$ meV]. Whereas electrons are repelled [Eq. (2′)] from the resulting potential barrier, the holes are attracted and trapped in the cubic crystallite [Eq. (2)] with a typical time constant of (τ_1). Here, as the Fermi level is in the conduction band, a large concentration of free electrons (5×10^{18} cm^{-3}) lead to very fast recombination [<1 ns, Eq. (3)]. As a result the number of electrons in the isolated cubic part is decreased and the remaining electron in the hexagonal matrix can contribute to the current because of its long lifetime. (No hole is left for recombination.) After several electrons have been removed from the cubic crystallite by this mechanism, the potential barrier is decreased and the electron capture rate is increased [Eq. (4)]. A dynamic equilibrium is reached, and the photocurrent saturates. After the light is switched off, the excess electrons in the hexagonal matrix are slowly captured into the cubic crystallites again. (τ_2) describes this relaxation time.

IV. SUMMARY

In summary we have studied optical sub-band-gap absorption in nominal hexagonal GaN films with PDS and CPM. A comparison of these measurement techniques is a very sensitive method for determining the energy dependence of $\eta\mu\tau$ and thus detecting small cubic inclusions, below the detection limit of ordinary x-ray diffraction, Raman scattering or transmission measurements. We also find deep acceptor levels in h-GaN at 220 and around 720 meV. A simple model is presented to explain the observed differences in PDS and CPM spectra. A correlation with temperature-dependent photoluminescence excited below and above the hexagonal band gap confirms our model. In agreement with Ref. 28, we attribute the photoluminescence lines at 3.313 and 3.369 eV, seen by many research

groups[6,21,23,31] in nominally hexagonal GaN, to near-band-gap luminescence of small cubic crystallites. These lines occur particularly in cubic samples where the Fermi level is in the conduction band. For small isolated crystals embedded in a nominally undoped hexagonal matrix, this condition is rather likely. These cubic crystallites are an effective sink for minority carriers that can lead to a persistent photoconductivity in *n*-type GaN.

ACKNOWLEDGMENTS

The authors would like to thank C. E. Nebel, M. S. Brandt, and M. Kelly for helpful discussions and suggestions. This work was supported by the Deutsche Forschungsgemeinschaft (Stu 139/3) and the Bayerische Kultusministerium [IX/2-52C(12)-61/27/87107].

[1] J. C. Zolper, R. J. Shul, A. G. Baca, R. G. Wilson, S. J. Pearton, and R. A. Stall, Appl. Phys. Lett. **68**, 2273 (1996).
[2] J. Burm, W. Schaff, L. F. Eastman, H. Amano, and I. Akasaki, Appl. Phys. Lett. **68**, 2849 (1996).
[3] M. A. Kahn, Q. Chen, C. J. Sun, J. W. Yang, M. S. Shur, and H. Park, Appl. Phys. Lett. **68**, 514 (1996).
[4] S. Nakamura, M. Senoh, S. Nagahama, N. Iwasa, T. Yamada, T. Matsushita, H. Kiyoku, and Y. Sugimoto, Appl. Phys. Lett. **68**, 3269 (1996).
[5] M. A. Kahn, J. N. Kuznia, D. T. Olson, J. M. Van Hove, M. Blasinggame, and L. F. Reitz, Appl. Phys. Lett. **60**, 2917 (1996).
[6] J. I. Pankove, J. E. Berkeyheiser, H. P. Maruska, and J. Wittke, Solid State Commun. **8**, 1051 (1970).
[7] R. Dingle, D. D. Sell, S. E. Stokowski, and M. Ilegems, Phys. Rev. B. **4**, 1211 (1971).
[8] B. Monemar, Phys. Rev. B **10**, 676 (1973).
[9] O. Lagerstedt and B. Monemar, J. Appl. Phys. **45**, 2266 (1974).
[10] W. J. Choyke and I. Linkov, in *The 5th SiC and Related Materials Conference, Washington, D.C., 1993*, IOP Conf. Proc. No. 137 (Institute of Physics, London, 1994), p. 141.
[11] M. R. H. Kahn, Y. Ohshita, N. Sawaki, I. Akasaki, Solid State Commun. **57**, 405 (1986).
[12] W. Götz, N. M. Johnson, R. A. Street, H. Amano, and I. Akasaki, Appl. Phys. Lett. **66**, 1340 (1995).
[13] P. Hacke, H. Nakayama, T. Detchprohm, K. Hiramatsu, and N. Sawaki, Appl. Phys. Lett. **68**, 1362 (1996).
[14] E. R. Glaser, T. A. Kennedy, K. Doverspike, L. B. Rowland, D. K. Gaskill, J. A. Freitas, M. A. Kahn, D. T. Olson, J. N. Kuzina, and D. K. Wickenden, Phys. Rev. B **51**, 13 326 (1995).
[15] O. Ambacher, W. Rieger, P. Ansmann, H. Angerer, T. D. Moustakas, and M. Stutzmann, Solid State Commun. **97**, 365 (1996).
[16] E. Rohrer, C. F. O. Graeff, R. Janssen, C. E. Nebel, and M. Stutzman, Phys. Rev. B (to be published).
[17] M. Vanecek, A. Abraham, O. Stika, J. Stuchlik, and J. Kocka, Phys. Status Solidi A **83**, 617 (1984).
[18] H. G. Grimmeiss and L. A. Lebedo, J. Appl. Phys. **46**, 2155 (1975).
[19] O. Ambacher, R. Dimitrov, D. Lentz, T. Metzger, W. Rieger, and M. Stutzmann, J. Cryst. Growth **167**, 1 (1996).
[20] A. C. Boccara, D. Fournier, W. B. Jackson, and N. M. Amer, Opt. Lett. **5**, 377 (1980).
[21] W. B. Jackson, N. M. Amer, A. C. Boccara, and D. Fournier, Appl. Opt. **20**, 1333 (1981).
[22] H. Siegle, L. Eckey, A. Hoffmann, C. Thomsen, B. K. Meyer, D. Schikora, M. Hankeln, K. Lischka, Solid State Commun. **96**, 943 (1995).
[23] B. K. Meyer, D. Volm, A. Graber, H. C. Alt, T. Detchprom, A. Amano, and I. Akasaki, Solid State Commun. **95**, 597 (1995).
[24] T. Matsumoto and M. Aoki, Jpn. J. Appl. Phys. **13**, 1804 (1974).
[25] S. Fischer, C. Wetzel, E. E. Haller, and B. K. Meyer, Appl. Phys. Lett. **67**, 1298 (1995).
[26] T. Ogino, M. Aoki, Jpn. J. Appl. Phys. **19**, 2395 (1980).
[27] C. Wetzel, S. Fischer, J. Krüger, E. E. Haller, R. J. Molnar, T. D. Moustakas, E. N. Mokhov, and P. G. Baranov, Appl. Phys. Lett. **68**, 2556 (1996).
[28] C. H. Hong, D. Pavlidis, S. W. Brown, and S. C. Rand, J. Appl. Phys. **77**, 1705 (1995).
[29] S. Strite, M. E. Lin, and H. Morkoc, Thin Solid Films **231**, 197 (1993).
[30] G. Ramirez-Flores, H. Navarro-Contreras, A. Lastras-Martinez, R. C. Powell, and J. E. Greene, Phys. Rev. B **50**, 8433 (1994).
[31] S. Logothetidis, J. Petalas, M. Cardona, and T. D. Moustakas, Phys. Rev. B **50**, 18 017 (1994).
[32] Y. G. Shreter and Y. T. Rebane (unpublished).
[33] D. C. Look, Z. Q. Fang, W. Kim, Ö. Aktas, A. Botchkarev, A. Salvador, and H. Morkoc, Appl. Phys. Lett. **68**, 3775 (1996).
[34] H. J. Queisser and D. E. Theodorou, Phys. Rev. B **33**, 4027 (1986).